Effects of vectorlike leptons on $h \to 4\ell$ and the connection to the muon $g-2$ anomaly.

Radovan Dermíšek,* Aditi Raval,† and Seodong Shin‡

Physics Department, Indiana University, Bloomington, IN 47405, USA

(Dated: June 25, 2014)

arXiv:1406.7018v2 [hep-ph] 24 Aug 2014

Abstract

The mixing of new vectorlike leptons with leptons in the standard model can generate flavor violating couplings of h, W and Z between heavy and light leptons. Focusing on the couplings of the muon, the partial decay width of $h \to e_4^\pm \mu^\mp$, where e_4 is the new lepton, can be significant when this process is kinematically allowed. Subsequent decays $e_4^\pm \to Z\mu^\pm$ and $e_4^\pm \to W^\pm \nu$ lead to the same final states as $h \to ZZ^* \to Z\mu^+\mu^-$ and $h \to WW^* \to W\mu\nu$, thus possibly affecting measurements of these processes. We calculate $h \to e_4\ell_i \to Z\ell_i\ell_j$, where $\ell_{i,j}$ are standard model leptons, including the possibility of off-shell decays, interference with $h \to ZZ^* \to Z\ell_i\ell_i$, and the mass effect of $\ell_{i,j}$ which are important when the mass of e_4 is close to the mass of the Higgs boson. We derive constraints on masses and couplings of the heavy lepton from the measurement of $h \to 4\ell$. We focus on the couplings of the muon and discuss possible effects on $h \to ZZ^*$ from the region of parameters that can explain the anomaly in the measurement of the muon $g-2$.

*dermisek@indiana.edu

†adiraval@indiana.edu

‡shinseod@indiana.edu

I. INTRODUCTION

Among simple extensions of the standard model (SM) are those with extra vectorlike fermions near the electroweak scale. Vectorlike fermions can acquire masses independently of their Yukawa couplings to the Higgs boson and thus are not strongly constrained (compared to chiral fermions) by experiments. However, even small Yukawa couplings between SM fermions and vectorlike fermions can affect a variety of processes, including Higgs boson decays.

We consider the extension of the SM with extra SU(2) doublet, L_L, and singlet, E_R, leptons (with the same hypercharges as SM leptons) and their vectorlike partners. The mixing of new vectorlike leptons with leptons in the SM can generate flavor violating couplings of h, W and Z between heavy and light leptons. Focusing on the couplings of the muon, the partial decay width of $h \to e_4^\pm \mu^\mp$, where e_4 is the lightest new mass eigenstate, can be significant if this process is kinematically allowed. Subsequent decays of the heavy lepton, $e_4^\pm \to Z\mu^\pm$ and $e_4^\pm \to W^\pm \nu$, lead to the same final states as $h \to ZZ^* \to Z\mu^+\mu^-$ and $h \to WW^* \to W\mu\nu$, thus possibly affecting measurements of these processes. Since the partial width of $h \to Z\mu^+\mu^-$ is much smaller than $h \to W\mu\nu$ in the SM, we mainly focus on $e_4^\pm \to Z\mu^\pm$.

We calculate $h \to e_4\ell_i \to Z\ell_i\ell_j$, where $\ell_{i,j}$ are SM leptons, including the possibility of off-shell decays, interference with $h \to ZZ^* \to Z\ell_i\ell_i$, and the mass effect of $\ell_{i,j}$ which are important when the mass of e_4 is close to the mass of the Higgs boson. We derive constraints on masses and couplings of the heavy lepton from the searches for $h \to ZZ^* \to 4\ell$ at ATLAS [1] and CMS [2].

Although our calculation is general and can be presented for any final state, we focus on the couplings of the muon and discuss possible effects on $h \to ZZ^* \to 4\mu$ or $2e2\mu$ from the region of parameters that can explain the anomaly in the measurement of the muon $g-2$. It has been shown that the discrepancy between the measured value of the muon anomalous magnetic moment and the SM prediction can be explained by contributions from extra vectorlike leptons [3, 4]. A particularly interesting solution to the muon $g-2$ simultaneously explaining the muon mass completely from the mixing of the muon with vectorlike leptons requires the mass of the lepton doublet to be within about 130 GeV [4]. Thus in a large range of the parameter space this solution predicts the existence of e_4 below

the Higgs mass and thus $h \to e_4^\pm \mu^\mp$ could be kinematically open and potentially significant. The $e_4 - \mu - h$, $e_4 - \nu - W$ and $e_4 - \mu - Z$ couplings needed to explain the muon $g-2$ anomaly are sufficient to modify the Higgs decays in 4ℓ and $2\ell 2\nu$ channels. Thus the contributions to the muon $g-2$ and $h \to 4\ell$ can be connected without any further assumptions. The correlation with contributions to other Higgs decays, $h \to \mu^+\mu^-$ and $h \to \gamma\gamma$, can be also found in [4].

Flavor violating Higgs decays into pairs of SM fermions were previously studied in Refs. [5, 6]. These can also be induced by mixing of SM fermions with vectorlike fermions; however, we do not consider this possibility here. We only allow one of the SM leptons to mix with vectorlike leptons in which case the flavor violating couplings to SM leptons are not generated.

In general, vectorlike quarks and leptons near the electroweak scale provide very rich phenomenology. For a recent discussion see for example Ref. [7] and references within. The addition of three or more complete vectorlike families also provides a simple UV completion of the SM featuring gauge coupling unification, sufficiently stable proton, and the Higgs quartic coupling remaining positive all the way to the grand unified theory (GUT) scale [8, 9].

This paper is organized as follows. In Sec. II, we briefly summarize the general framework and discuss constraints on possible flavor violating couplings between the muon and a heavy lepton. In Sec. III, we calculate the effect of $h \to e_4^\pm \mu^\mp \to Z\mu^+\mu^-$ on $h \to 4\ell$. We also discuss a connection with the explanation of the muon $g-2$ anomaly in Sec. IV and provide some concluding remarks in Sec. V. In Appendixes we extract bounds on $h \to 4\mu$ and $h \to 2e2\mu$ from ATLAS and CMS searches, compare the ATLAS and CMS limits on couplings and masses of the new lepton, and calculate the partial width of a scalar to four leptons in the presence of general flavor violating couplings of the new lepton. These formulas include the mass effects of final state leptons and interference with $h \to ZZ^*$. We also briefly comment on the impact of constraints from $h \to WW^* \to 2\ell 2\nu$ which are typically weaker than those from $h \to ZZ^* \to 4\ell$, unless $\mathrm{BR}(e_4^\pm \to W^\pm \nu)$ is close to 1.

II. OUTLINE OF THE FRAMEWORK

We extend the SM by vectorlike pairs of new leptons, $L_{L,R}$ and $E_{L,R}$, where E_R (L_L) has the same quantum numbers as μ_R (μ_L) in the SM, and E_L (L_R) is its vectorlike partner. For

SU(2) doublets we use the same label for their charged components as for the whole doublets. We assume that the new leptons mix only with one SM lepton and we take the muon as an example. The results for the electron or tau lepton could be obtained in the same way. If the new leptons mix simultaneously with more than one SM lepton, the generated flavor violating couplings need to satisfy all the constraints from a variety of processes involving SM fermions. We will not pursue this direction here, and for simplicity we assume that all other couplings are zero.

With this assumption, the most general renormalizable Lagrangian for the muon and new leptons is given by:

$$\begin{aligned}\mathcal{L} \supset & -\bar{\mu}_L y_\mu \mu_R H - \bar{\mu}_L \lambda^E E_R H - \bar{L}_L \lambda^L \mu_R H - \lambda \bar{L}_L E_R H - \bar{\lambda} H^\dagger \bar{E}_L L_R \\ & - M_L \bar{L}_L L_R - M_E \bar{E}_L E_R + h.c., \end{aligned} \tag{1}$$

where the first term is the usual SM Yukawa coupling, followed by Yukawa couplings between the muon and vectorlike leptons, Yukawa couplings between vectorlike leptons, and mass terms for vectorlike leptons.

After spontaneous symmetry breaking, $H = (0, v + h/\sqrt{2})^T$, the resulting mass matrix for the muon and the extra leptons can be diagonalized by a biunitary transformation:

$$U_L^\dagger \begin{pmatrix} y_\mu v & 0 & \lambda^E v \\ \lambda^L v & M_L & \lambda v \\ 0 & \bar{\lambda} v & M_E \end{pmatrix} U_R = \begin{pmatrix} m_\mu & 0 & 0 \\ 0 & m_{e_4} & 0 \\ 0 & 0 & m_{e_5} \end{pmatrix}, \tag{2}$$

where we label the new mass eigenstates by e_4 and e_5.

Couplings of the muon and heavy leptons to the Z, W and Higgs bosons are modified because the E_L is an SU(2) singlet mixing with other SU(2) doublets, and the charged component of L_R which originates from an SU(2) doublet mixes with other SU(2) singlets. The flavor conserving couplings receive corrections and flavor violating couplings between the muon and heavy leptons are generated. These couplings are given in Ref. [4] in terms of diagonalization matrices. The forms of diagonalization matrices $U_{L,R}$, which are useful for deriving approximate formulas for couplings of Z, W and h, are also given in Ref. [4] in the limit $\lambda^E v, \lambda^L v, \bar{\lambda} v, \lambda v \ll M_E, M_L$.

In what follows we assume that only one new lepton is below or close to the Higgs mass and we define the couplings of the lighter new lepton, e_4, and the muon to the Z and Higgs

bosons by the effective Lagrangian of the form

$$\mathcal{L} \supset\ g_L^Z\, \bar{e}_{4L}\gamma^\mu \mu_L Z_\mu\ +\ g_R^Z\, \bar{e}_{4R}\gamma^\mu \mu_R Z_\mu\ -\ \frac{1}{\sqrt{2}} g_R^h\, \bar{e}_{4L}\mu_R h\ -\ \frac{1}{\sqrt{2}} g_L^h\, \bar{e}_{4R}\mu_L h\ + h.c.. \qquad (3)$$

The formulas for these couplings, and all other couplings (couplings to W and flavor conserving couplings) in terms of Lagrangian parameters can be found in Ref. [4].

In order to satisfy precision electroweak data related to the muon that include the Z pole observables (Z partial width, forward-backward asymmetry, left-right asymmetry), the W partial width, the muon lifetime and constraints from oblique corrections, namely from S and T parameters, possible values of g_L^Z and g_R^Z are constrained to be smaller than about 0.01 and 0.015. The maximum allowed values of the Higgs couplings depend on the size of the Yukawa couplings in Eq. (1). Limiting all couplings to be smaller than 0.5 (1.0) the g_L^h coupling is limited to 0.03 (0.06) and the g_R^h coupling is limited to 0.04 (0.08). We also impose the LEP limit, 105 GeV, on the mass of the new charged lepton.

III. $h \to e_4^\pm \mu^\mp \to Z\mu^+\mu^-$ AND $h \to ZZ^* \to Z\mu^+\mu^-$

Even a small flavor violating coupling of the Higgs boson to a new charged lepton and the muon can lead to a sizable contribution to the Higgs width if $h \to e_4^\pm \mu^\mp$ is kinematically open. The decay mode of the new lepton, $e_4^\pm \to Z\mu^\pm$, leads to $h \to Z\mu^+\mu^-$ final state (see Fig. 1), which is the same as the final state of $h \to ZZ^* \to Z\mu^+\mu^-$. Thus the new charged lepton can contribute to the $h \to 4\mu$ and $h \to 2e2\mu$ processes. Without additional couplings it cannot contribute to $h \to 2\mu 2e$ (the first pair of leptons originating from the on-shell Z) or $h \to 4e$ decay modes.

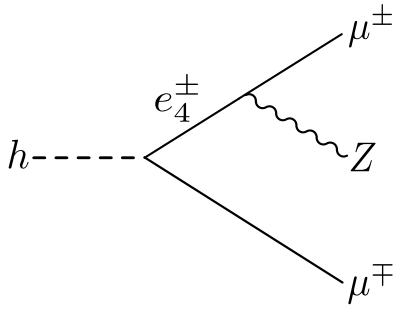

FIG. 1: The Feynman diagram for $h \to e_4^\pm \mu^\mp \to Z\mu^+\mu^-$ contributing to the same final state as $h \to ZZ^* \to Z\mu^+\mu^-$.

The approximate formula for the partial decay width of $h \to e_4^\pm \mu^\mp$, neglecting the mass of the muon, is given by

$$\Gamma(h \to e_4^\pm \mu^\mp) \simeq \frac{m_h}{16\pi} \left[(g_L^h)^2 + (g_R^h)^2 \right] \left(1 - \frac{m_{e_4}^2}{m_h^2} \right)^2 \tag{4}$$

and the formula for $e_4^\pm \to Z\mu^\pm$ in the same approximation is given by

$$\Gamma(e_4^\pm \to Z\mu^\pm) = \frac{m_{e_4}}{32\pi} \left[(g_L^Z)^2 + (g_R^Z)^2 \right] \frac{m_{e_4}^2}{M_Z^2} \left(1 - \frac{M_Z^2}{m_{e_4}^2} \right)^2 \left(1 + 2\frac{M_Z^2}{m_{e_4}^2} \right). \tag{5}$$

The complete formula for $h \to (e_4^\pm \mu^\mp, ZZ^*) \to Z\mu^+\mu^-$ and actually for any fermions in the final state, including the mass effect of final state fermions, the contribution from off-shell e_4 and the interference with $h \to ZZ^*$ is given in Appendix C.

Although the 4ℓ final states originating from $h \to e_4^\pm \mu^\mp$ and $h \to ZZ^*$ are identical, the kinematical distribution of final state leptons is not. The muon that accompanies the e_4 is somewhat soft, and if the mass of e_4 is close to the Higgs mass, this muon does not pass the cuts used in the $h \to ZZ^*$ analysis. To quantify the contribution of the $h \to e_4^\pm \mu^\mp$ to $h \to Z\mu^+\mu^-$ we define

$$R_{Z\mu\mu} = \xi \frac{\Gamma(h \to (e_4^\pm \mu^\mp, ZZ^*) \to Z\mu^+\mu^-)}{\Gamma(h \to ZZ^* \to Z\mu^+\mu^-)_{SM}}, \tag{6}$$

where ξ is the acceptance of the SM+new lepton contribution to $h \to Z\mu^+\mu^-$ relative to the SM $h \to ZZ^* \to Z\mu^+\mu^-$. Because of the interference the contributions from new physics and the SM do not factor out.

The relative acceptance for $h \to 4\mu$ case is given in Fig. 2 as a function of the mass of the e_4 for various values of g_L^h coupling. We adopt the cuts from the ATLAS analysis [1]. For sizable g_L^h coupling the $h \to e_4^\pm \mu^\mp$ would easily dominate over $h \to Z\mu^+\mu^-$. As the mass of the e_4 increases, the accompanying muon is getting softer and eventually does not pass the cuts in the $h \to ZZ^*$ analysis. Thus, the acceptance is dropping significantly at about 6 GeV from the Higgs mass. Close to the kinematical threshold it increases again since the SM contribution dominates. As the g_L^h coupling decreases, the SM contribution starts to dominate and the relative acceptance is getting close to 1. The g_L^Z coupling is set to 0.01 and other couplings are set to zero in Fig. 2. The results do not depend much on the choice of g_L^Z since it only enters through the interference with the SM contribution or when the e_4 is not on shell. The results for other coupling combinations are almost identical since the interference is small (the interference changes sign when $g_L^Z \leftrightarrow g_R^Z$).

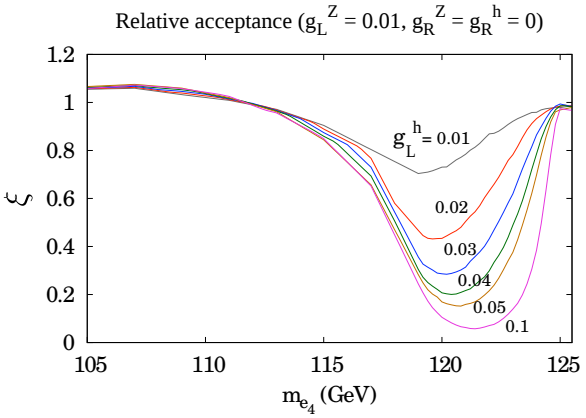

FIG. 2: The Atlas acceptance of $h \to (e_4^{\pm}\mu^{\mp}, ZZ^*) \to 4\mu$ relative to the $h \to ZZ^* \to 4\mu$ in the SM.

Predictions for $R_{Z\mu\mu}$ as a function of g_L^h and m_{e_4} for fixed $g_L^Z = 0.01$ and $g_R^h = g_R^Z = 0$ are given in Fig. 3. The thick line represents the ATLAS upper exclusion limit for 4μ final state, which is discussed in detail in Appendix A. The plots assume $\mathrm{BR}(e_4 \to Z\mu) = 100\%$. For smaller $\mathrm{BR}(e_4 \to Z\mu)$ predicted values of $R_{Z\mu\mu}$ and the exclusion limit can be obtained by simple rescaling. As is easily seen a large region of possible couplings and masses of the e_4 is excluded. However, for $m_{e_4} \gtrsim 120$ GeV the $h \to 4\mu$ does not exclude any scenario that would not be already excluded by precision electroweak (EW) data.

Defining the average Higgs coupling,

$$g_h \equiv \sqrt{(g_L^h)^2 + (g_R^h)^2}, \tag{7}$$

which approximately controls the partial width of $h \to e_4^{\pm}\mu^{\mp}$, the y-axis of the plots in Fig. 3 could be very well approximated by $g_h\sqrt{\mathrm{BR}(e_4 \to Z\mu)}$ when e_4 is on-shell.

IV. CONNECTION WITH THE MUON $g-2$ ANOMALY

The discrepancy between the measured value of the muon anomalous magnetic moment [10] and the SM prediction, $\Delta a_\mu^{exp} = a_\mu^{exp} - a_\mu^{SM} = 2.7 \pm 0.80 \times 10^{-9}$, is at the level of 3.4 standard deviations. It can be explained by contributions from extra charged lepton (originating either from L and E) in the loop diagram with the Higgs and Z bosons, and extra neutrino (originating from L) in the loop diagram with the W boson [3][4].

In Ref. [4] it was shown that there are two generic solutions to the muon $g-2$ that differ in the correlation between the contribution of the vectorlike leptons to the muon mass, m_μ^{LE},

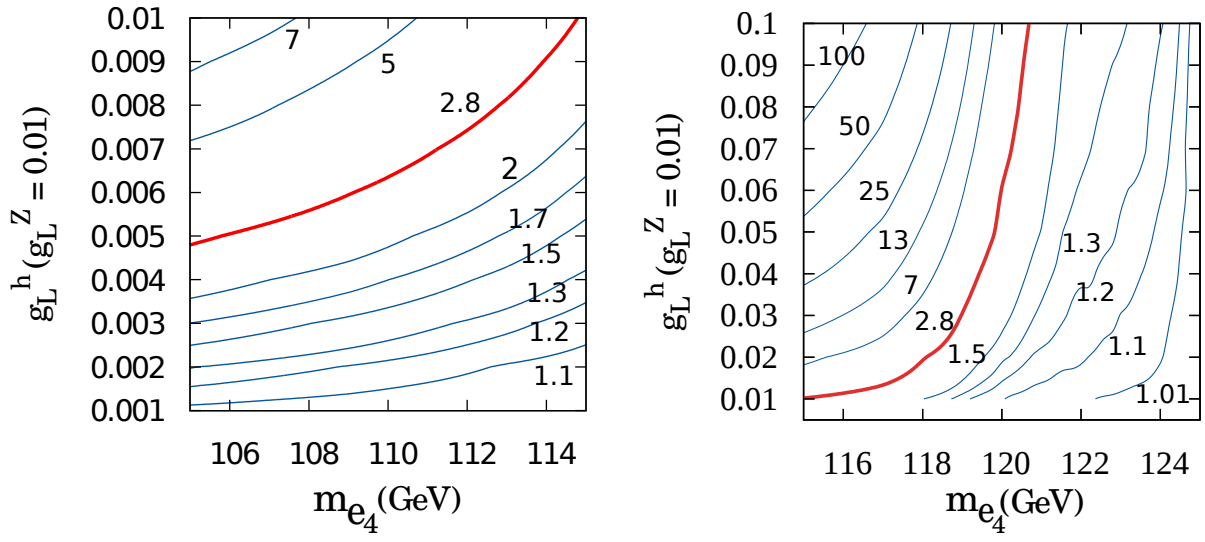

FIG. 3: Contours of constant $R_{Z\mu\mu}$ in $g_L^h - m_{e_4}$ plane for fixed $g_L^Z = 0.01$ and $g_R^h = g_R^Z = 0$ assuming BR$(e_4 \to Z\mu) = 100\%$. The thick line represents the ATLAS exclusion limit for 4μ final state. For smaller BR$(e_4 \to Z\mu)$ predicted values of $R_{Z\mu\mu}$ and the exclusion limit can be obtained by simple rescaling.

and the muon $g-2$. This correlation is controlled by M_L which represents the mass of extra neutrino ν_4. In the asymptotic solution, $M_L \gg M_Z$, the Higgs loop dominates and the measured value of the muon $g-2$ is obtained for $m_\mu^{LE}/m_\mu \simeq -1$. In this case, the physical muon mass is a result of a cancellation between twice as large direct Yukawa coupling and the contribution from the mixing with heavy leptons. The second solution is with a light extra neutrino, $M_L \simeq M_Z$, in which case the W loop dominates and the measured value of the muon $g-2$ is obtained for $m_\mu^{LE}/m_\mu \simeq +1$. In this case, the muon mass can fully originate from the mixing with heavy leptons.

The sizes of possible contributions from vectorlike leptons to various observables depend on the upper limit on Yukawa couplings that we allow in the model. The upper limit 0.5 is sufficient to fully explain the muon $g-2$ anomaly and generate the muon mass and is small enough so that the model can be embedded into a scenario with three complete vectorlike families which provides a simple UV embedding (with gauge coupling unification, sufficiently stable proton, and the Higgs quartic coupling remaining positive all the way to the GUT scale) [8, 9]. With this upper limit, the muon $g-2$ can be explained within one standard deviation with $M_L \lesssim 130$ GeV and the mass of the lightest extra charged lepton originating mostly from L, $m_{e_4} \lesssim 150$ GeV. The mass of e_4 is not strictly given by M_L due to possible

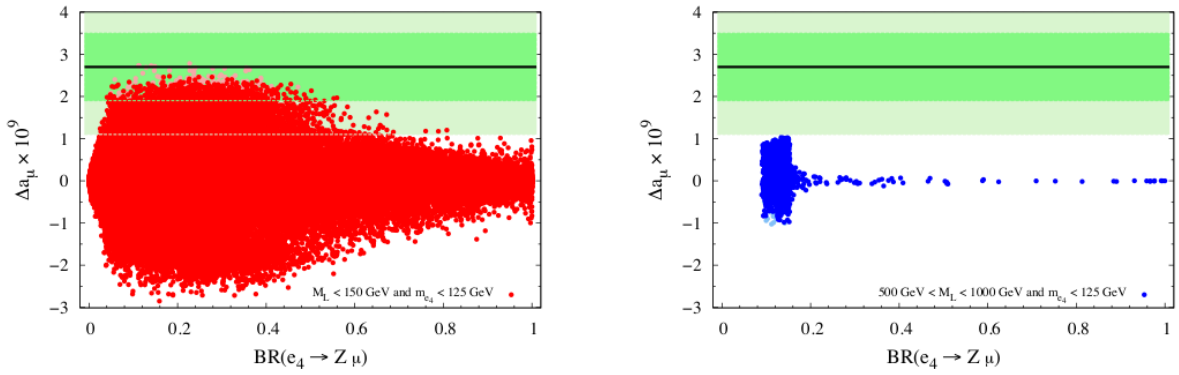

FIG. 4: Randomly generated points with $M_L \in [100, 150]$ GeV (left) and $M_L \in [500, 1000]$ GeV (right), with $M_E \in [100, 1000]$ GeV, $\lambda,\ \bar{\lambda} < 0.5$, and $\lambda^{L,E}$ in allowed ranges from precision EW data, plotted in Δa_μ – BR($e_4 \to Z\mu$) plane. The lightest mass eigenstate is required to satisfy the LEP limit. This is a subset of the points generated in Ref. [4] which have one mass eigenstate below the Higgs mass 125 GeV. The lightly shaded points are excluded by the CMS search for $h \to \mu^+\mu^-$. The horizontal line and dark (light) shaded bands correspond to the central experimental value of Δa_μ and 1σ (2σ) regions, respectively.

mixing. In about half of the allowed region the mass of e_4 is below the Higgs boson mass and thus $h \to e_4^\pm \mu^\mp$ can significantly contribute to $h \to 4\mu$ ($2e2\mu$). The asymptotic solution requires, $M_L \gtrsim 1$ TeV, but even in this case, the other charged lepton, originating mostly from E, can be below the Higgs mass. We will present results for both cases.

In this section, we use the same points in the parameter space generated for Ref. [4] so that the correlations with other observables studied in [4], $h \to \mu^+\mu^-$ or $h \to \gamma\gamma$, can be easily inferred. However, we impose new constraints on $h \to \mu^+\mu^-$ from CMS, which limit

$$R_{\mu\mu} \equiv \frac{\Gamma(h \to \mu^+\mu^-)}{\Gamma(h \to \mu^+\mu^-)_{SM}}. \tag{8}$$

to $R_{\mu\mu}^{exp} \leq 7.4$ [11]. It is interesting to note that there is a slight excess of events for the reconstructed dimuon mass near the measured Higgs mass. The small M_L solution to the muon $g-2$ predicts enhancement of the $h \to \mu^+\mu^-$ by a factor of 5 – 9.

In Figs. 4 and 5 we plot the contribution to the muon $g-2$ versus BR($e_4 \to Z\mu$) for the subset of the points generated in Ref. [4] which have one mass eigenstate below the Higgs mass, 125 GeV. Points with $M_L \in [100, 150]$ GeV are plotted on the left and those with $M_L \in [500, 1000]$ GeV are on the right. The lightly shaded points show the impact of the

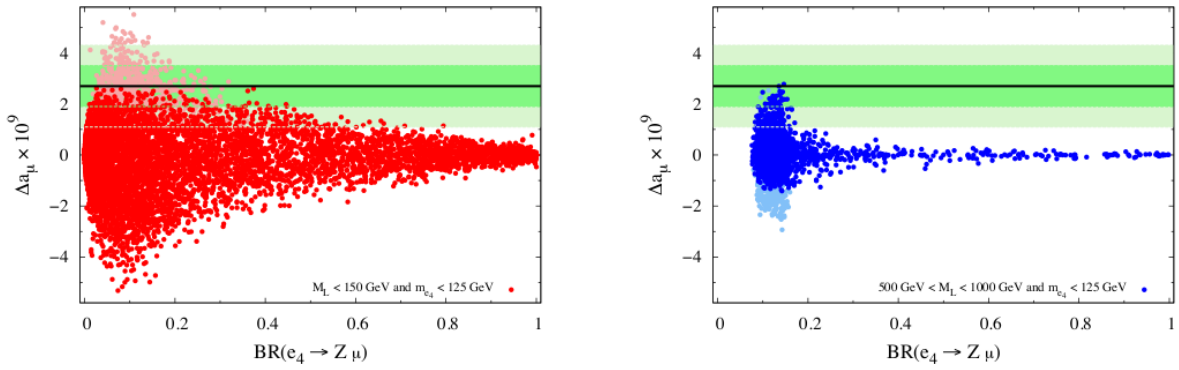

FIG. 5: The same as in Fig. 4 with ranges of Yukawa couplings λ, $\bar{\lambda}$ extended to 1.

CMS search for $h \to \mu^+\mu^-$. In Fig. 4 the Yukawa couplings in Eq. (1) are limited to 0.5, while in Fig. 5 their possible values are extended to 1. Precision EW data and the LEP limit on a new charged lepton mass, 105 GeV, are satisfied by all points. We see that the points that can explain the muon $g-2$ within 1 standard deviation predict BR($e_4 \to Z\mu$) between a few and 50% for the small M_L solution, and about 10% for the asymptotic case. The rest of the width of e_4 is given by $e_4 \to W\nu$, since e_4 cannot decay to the Higgs boson.

The correlation between BR($e_4 \to Z\mu$) and the average Higgs coupling g_h defined in Eq. (7) is shown in Figs. 6 and 7. The plotted points are all the points from Figs. 4 and 5 that satisfy the CMS limit on $h \to \mu^+\mu^-$. The darker points (orange points on the left and green points on the right) satisfy the muon $g-2$ within 2σ while the darkest points (dark red points on the left and dark blue points on the right) satisfy the muon $g-2$ within 1σ.

Finally, in Figs. 8 and 9 we show the same points in $g_h\sqrt{\text{BR}(e_4 \to Z\mu)}$ – m_{e_4} plane. The combination $g_h\sqrt{\text{BR}(e_4 \to Z\mu)}$ very well approximates the y axis of Fig. 3. This plot indicates that there are many scenarios which can explain the muon $g-2$ anomaly within 1 sigma and simultaneously significantly enhance $h \to 4\mu$. Limiting Yukawa couplings to 0.5, the mass of e_4 has to be larger than about 113 GeV in order not to be ruled out by $h \to 4\mu$. Increasing the Yukawa coupling up to 1, the m_{e_4}can be close to the LEP limit for the small M_L case. For the asymptotic case, m_{e_4} is required to be larger than about 119 GeV. Selected contours of constant $R_{Z\mu\mu}$ from Fig. 3 indicate the impact of improved limits in the future.

Predictions for $h \to 2e2\mu$ and limits from the ATLAS analysis in this channel are almost identical and thus we do not show them separately. The comparison of the impact of ATLAS

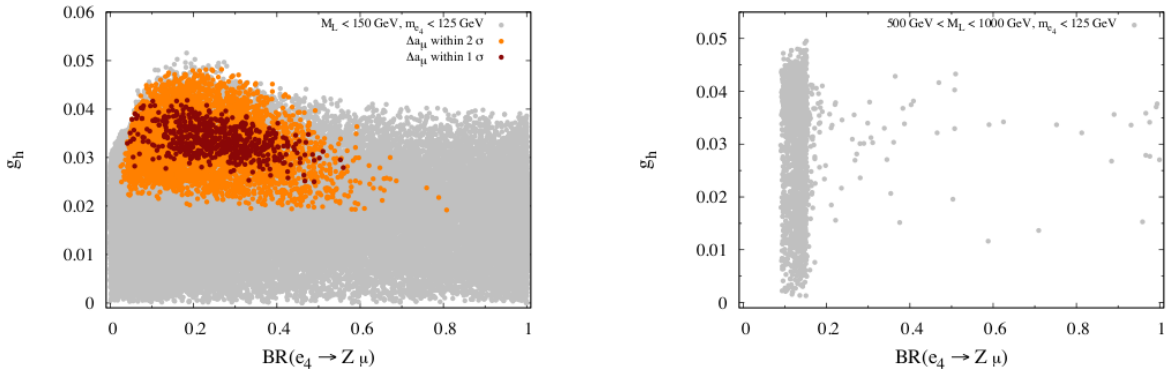

FIG. 6: Points from Fig. 4 that satisfy the CMS limit on $h \to \mu^+\mu^-$ plotted in g_h – BR($e_4 \to Z\mu$) plane. The darker points (orange points on the left) satisfy the muon $g-2$ within 2σ while the darkest points (dark red points on the left) satisfy the muon $g-2$ within 1σ.

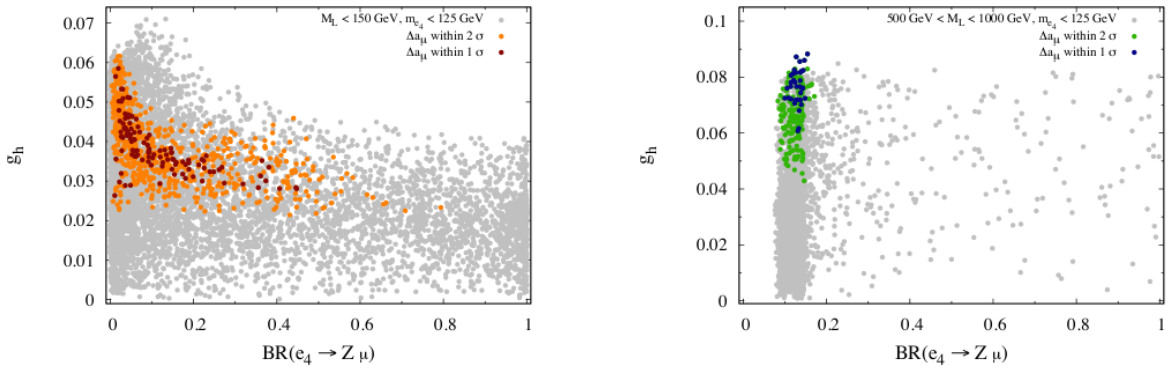

FIG. 7: Points from Fig. 5 that satisfy the CMS limit on $h \to \mu^+\mu^-$ plotted in g_h – BR($e_4 \to Z\mu$) plane. The darker points (orange points on the left and green points on the right) satisfy the muon $g-2$ within 2σ while the darkest points (dark red points on the left and dark blue points on the right) satisfy the muon $g-2$ within 1σ.

and CMS analyses is given in Appendix B for the $h \to 4\mu$ case. The CMS analysis does not separate $2e2\mu$ final states based on which pair of leptons originates from the on-shell Z, and thus the comparison in this channel is not possible.

In Appendix B we also briefly discuss constraints from $h \to WW^* \to 2\ell 2\nu$ on $h \to e_4^\pm \mu^\mp \to W^\pm \mu^\mp \nu$. We show that these constraints are weaker than those from $h \to ZZ^* \to 4\ell$, unless BR($e_4^\pm \to W^\pm \nu$) is close to 1.

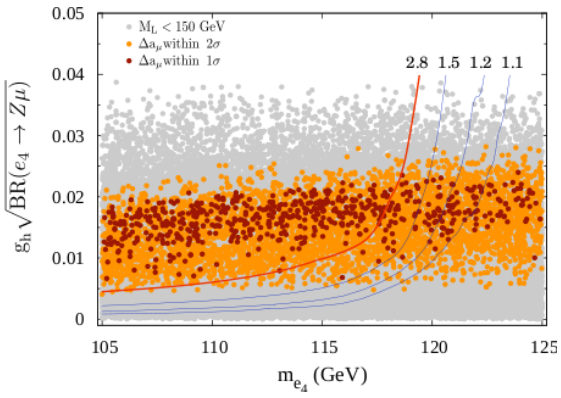

FIG. 8: Points from Fig. 4 (left) that satisfy the CMS limit on $h \to \mu^+\mu^-$ plotted in $g_h\sqrt{\mathrm{BR}(e_4 \to Z\mu)}$ – m_{e_4} plane. The darker (orange) points satisfy the muon $g-2$ within 2σ while the darkest (dark red) points satisfy the muon $g-2$ within 1σ. Overlaid are selected contours of constant $R_{Z\mu\mu}$ from Fig. 3.

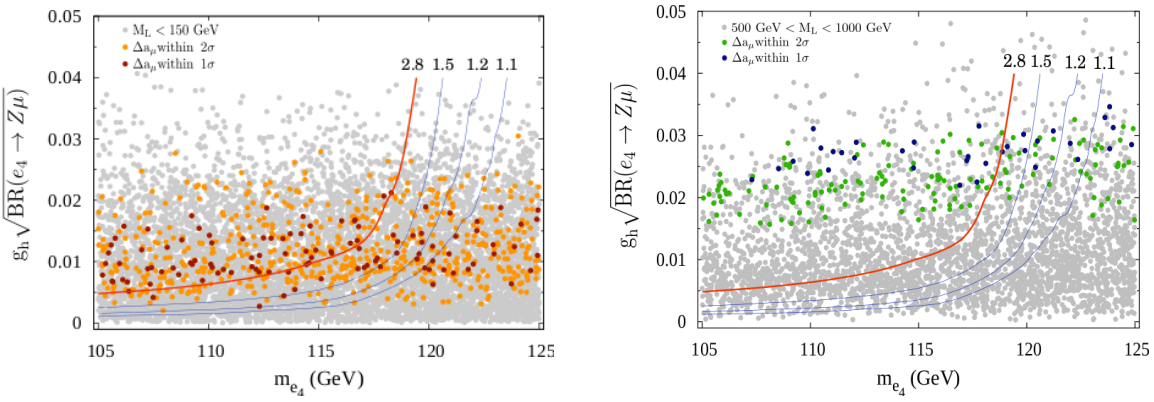

FIG. 9: Points from Fig. 5 that satisfy the CMS limit on $h \to \mu^+\mu^-$ plotted in $g_h\sqrt{\mathrm{BR}(e_4 \to Z\mu)}$ – m_{e_4} plane. The darker points (orange points on the left and green points on the right) satisfy the muon $g-2$ within 2σ while the darkest points (dark red points on the left and dark blue points on the right) satisfy the muon $g-2$ within 1σ. Overlaid are selected contours of constant $R_{Z\mu\mu}$ from Fig. 3.

V. DISCUSSION AND CONCLUSIONS

In extensions of the SM by vectorlike leptons the new lepton, e_4, may be lighter than the Higgs boson. Because of possible flavor violating couplings, $h \to e_4^\pm \mu^\mp$ with subsequent decays of the heavy lepton, $e_4^\pm \to Z\mu^\pm$, can significantly contribute to $h \to Z\mu^+\mu^-$ and thus affect the measurement of Higgs decays in 4μ or $2e2\mu$ final states.

We derived limits on couplings and the mass of the new lepton from ATLAS and CMS searches for $h \to 4\ell$. We focused on the couplings of the muon and discussed possible effects on $h \to ZZ^* \to 4\mu$ or $2e2\mu$ from the region of parameters that can explain the anomaly in the measurement of the muon $g-2$. Couplings required for the explanation of the muon $g-2$ also generate $h \to e_4^\pm \mu^\mp \to Z\mu^+\mu^-$. This scenario predicts equal enhancement of $h \to 4\mu$ and $2e2\mu$ (first pair of leptons originating from the on-shell Z) and no enhancement in $h \to 4e$ and $2\mu 2e$ final states. We showed that scenarios that can explain the muon $g-2$ within 1σ are typically ruled out by $h \to 4\mu$ for $m_{e_4} \lesssim 118$ GeV. However, there are some viable scenarios with lighter e_4, even close to the LEP limit. We also showed the impact of improved limits on $h \to ZZ^* \to 4\mu$ in future. However, if e_4 is heavier than the Higgs boson, its effect on Higgs decay is negligible while it can still explain the muon $g-2$. We also derived constraints from $h \to WW^* \to 2\ell 2\nu$ on $h \to e_4^\pm \mu^\mp \to W^\pm \mu^\mp \nu$. We showed that these constraints are weaker than those from $h \to ZZ^* \to 4\ell$, unless $\mathrm{BR}(e_4^\pm \to W^\pm \nu)$ is close to 1.

Vectorlike leptons can be pair produced at the LHC. Although $e_4^\pm \to Z\mu^\pm$ provides a very clean and distinctive signal, the rate for this decay mode might be small. The remaining decay mode, $e_4^\pm \to W^\pm \nu$, which can be dominant, is harder to constrain. In addition, the new leptons can also decay into τ leptons reducing the number of light leptons in final states. Compilation of constraints on vectorlike leptons from searches for anomalous production of multi lepton events can be found in Ref. [12].

Note added. During the completion of this work papers studying effects of new physics on $h \to 4\ell$ appeared. In Ref. [13], authors studied effects of new light scalar or vector fields, and in Ref. [14], the effects of light $SU(2)$ singlet vectorlike leptons were also considered.

Acknowledgments

We would like to thank J. Hall and E. Lunghi for useful discussions. R.D. also thanks H.D. Kim for discussions and Seoul National University and the Mainz Institute for Theoretical Physics (MITP) for their hospitality and partial support during the completion of this work. S.S. thanks the Deutsches Elektronen-Synchrotron (DESY, Hamburg) for the support of visit during the process of this work. This work was supported in part by the Department of

Energy under Grant NO. DE-FG02-13ER42002.

Appendix A: Limits on new physics contributing to $h \to Z\mu^+\mu^-$

In this Appendix we use ATLAS [1] and CMS [2] searches for $h \to ZZ^* \to 4\ell$ to derive the 95 % C.L. upper limits on new physics contribution to $h \to Z\mu^+\mu^-$ with Z further decaying into $\mu^+\mu^-$ or e^+e^-. We adopt a modified frequentist construction ($\mathrm{CL_s}$) [15] (see also Appendix D of [16]).

The expected number of $h \to 4\ell$ events after applying given selection cuts can be written as:

$$E = \eta \cdot \sigma^0 \cdot \mathcal{L} = \frac{\eta}{\eta_{\rm SM}} \cdot \frac{\sigma^0}{\sigma^0_{\rm SM}} \cdot E_{\rm SM} = \xi \cdot \frac{\sigma^0}{\sigma^0_{\rm SM}} \cdot E_{\rm SM} \ , \tag{A1}$$

where η is the cut efficiency, σ^0 is the cross section that includes both the SM $h \to 4\ell$ and the new physics contribution before the cuts, and $\mathcal{L}$ is the integrated luminosity. The $\eta_{\rm SM}$, $\sigma^0_{\rm SM}$, and $E_{\rm SM}$ are the cut efficiency for the SM contribution only, the SM cross section before the cuts, and the expected number of the SM $h \to ZZ^* \to 4\ell$ events, respectively. Finally, ξ is the relative cut acceptance $\eta/\eta_{\rm SM}$. The upper limit on $\sigma^0/\sigma^0_{\rm SM}$ can be obtained by constraining the expected number of events E to be smaller than the 95 % $\mathrm{CL_s}$ limit, ℓ_{95}, obtained (below) from experiments,

$$\sigma^0/\sigma^0_{\rm SM} < \frac{\ell_{95}}{\xi \cdot E_{\rm SM}} \ . \tag{A2}$$

Equivalently, we can obtain a limit on

$$\mu \equiv \sigma/\sigma_{\rm SM} = \xi\sigma^0/\sigma^0_{\rm SM} < \frac{\ell_{95}}{E_{\rm SM}} \ , \tag{A3}$$

where the cross sections σ and $\sigma_{\rm SM}$ are those after applying the cuts. This quantity is related to $R_{Z\mu\mu}$, defined in Eq. (6):

$$R_{Z\mu\mu} = \xi \cdot \frac{\Gamma_h^{\rm tot}}{\Gamma_h^{\rm SM}} \cdot \frac{\sigma^0}{\sigma^0_{\rm SM}} = \mu \cdot \frac{\Gamma_h^{\rm tot}}{\Gamma_h^{\rm SM}} \tag{A4}$$

in the region of the parameter space where the narrow width approximation works well. Here, $\Gamma_h^{\rm tot}$ is the total decay width of the Higgs boson which includes possible decay mode to a new lepton, while $\Gamma_h^{\rm SM} = 4.07$ MeV is the SM expectation [17].

In the modified frequentist construction, a confidence level $1-\alpha$ is obtained by the ratio of probabilities:

$$\alpha = \frac{P(D \geq \lambda|_{H_0})}{P(D \geq \lambda|_{H_1})} \ , \tag{A5}$$

where D is the data and λ is the expected distribution in the signal-plus-background (H_0) and in the background-only (H_1) hypotheses. The signal-plus-background is given by

$$S + B = s + b \pm \sqrt{s + \Sigma^2 s^2 + b + \sigma_b^2} \ , \tag{A6}$$

where s is the expected signal with statistical uncertainty $\sqrt{s}$. We assume that the fractional systematic uncertainties Σ are the same as those in the SM $h \to ZZ^* \to 4\ell$ searches at 8 TeV.[1] The expected background is b with statistical uncertainty $\sqrt{b}$ and systematic uncertainty σ_b [1, 2]. Assuming every distribution is Gaussian we can take

$$P(D \geq \lambda|_{H_0}) \ = \ \Phi\left(\frac{D - s - b}{\sqrt{s + \Sigma^2 s^2 + b + \sigma_b^2}}\right) \ , \tag{A7}$$

$$P(D \geq \lambda|_{H_1}) \ = \ \Phi\left(\frac{D - b}{\sqrt{b + \sigma_b^2}}\right) \ , \tag{A8}$$

where Φ is the cumulative distribution function. For a given set of D, b, Σ, σ_b, and α the $1 - \alpha$ confidence level limit is obtained from Eq. (A5). Setting $\alpha = 0.05$ we obtain the 95 % C.L. limit, ℓ_{95}.

In our analysis, in order to obtain the limits we include the SM $h \to ZZ^* \to 4\mu$ ($2e2\mu$) process in the signal. The upper bounds on $\mu = \sigma/\sigma_{\rm SM}$ as the 95% C.L. limits from both ATLAS and CMS data are shown in Table I. The ATLAS limits are from 4.6 and 20.7 fb^{-1} at $\sqrt{s} = 7$ TeV and $\sqrt{s} = 8$ TeV respectively [1], while the CMS limits are from 5.1 and 19.5 fb^{-1} at $\sqrt{s} = 7$ TeV and $\sqrt{s} = 8$ TeV respectively [2]. We do not include $2e2\mu$ final state for the CMS since they do not separate $2e2\mu$ and $2\mu2e$ data ($2e$ originating from on-shell or off-shell Z).

TABLE I: The 95% CL$_{\rm s}$ exclusion bound on $\mu \equiv \sigma/\sigma_{\rm SM}$, which is $\ell_{95}/E_{\rm SM}$.

	ATLAS 7+8 TeV 4.6+20.7 fb^{-1}	CMS 7+8 TeV 5.1 + 19.5 fb^{-1}
4μ	2.85	1.85
$2e2\mu$	3.02	No separate $2e$ from on-shell Z

During the completion of this work a new ATLAS $h \to 4\ell$ analysis appeared [18] based on 20.3 and 4.5 fb^{-1} data at 8 and 7 TeV, respectively. Because of effective discrimination

[1] For the 4μ final state these are 11.4% at ATLAS [1] and 11.9% at CMS [2]. For $2e2\mu$ final state at ATLAS it is 11.6%.

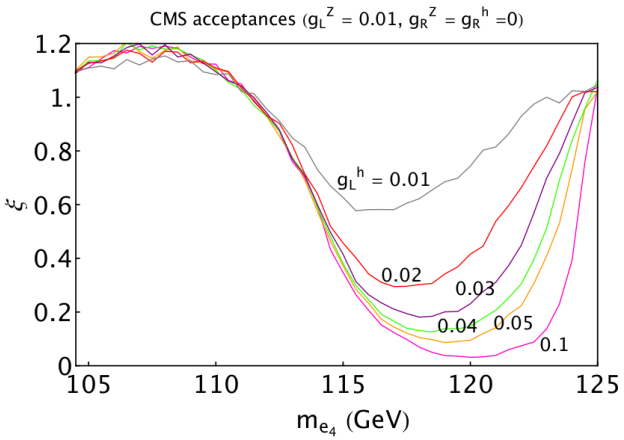

FIG. 10: The CMS acceptance of $h \to (e_4^\pm \mu^\mp, ZZ^*) \to 4\mu$ relative to the $h \to ZZ^* \to 4\mu$ in the SM.

of $J/\psi \to \ell^+\ell^-$ the number of observed events slightly increased. However, the bounds are similar to those in Table I: 3.04 for 4μ and 3.28 for $2e2\mu$.

Appendix B: Details of the analysis and comparison of ATLAS and CMS

The relative acceptances, ξ, are obtained using MadGraph 5 [19] for simulating the process $gg \to h \to Z\mu^+\mu^-$ with subsequent decay of $Z \to \mu^+\mu^-$ or e^+e^- from the model written with FeynRules [20]. We also used Pythia 6 [21] to include the initial and final state radiation. The production processes include the new physics $gg \to h \to e_4^\pm \mu^\mp \to 4\mu$ $(2e2\mu)$, the SM $gg \to h \to ZZ^* \to 4\mu$ $(2e2\mu)$, and their interference. The relative acceptances for the ATLAS analysis for selected values of couplings were given in Fig. 2 and, for comparison, the corresponding acceptances for the CMS analysis are given in Fig. 10. In this figure we assume $\mathrm{BR}(e_4^\pm \to Z\mu^\pm) = 1$. The decay width of the Higgs boson is calculated including the new process $h \to e_4^\pm \mu^\mp$. The dependence of ξ on the mass of the new lepton and the g_L^h coupling is very similar to the ATLAS case.

The predicted cross section σ^0 for 4μ final state is shown in Fig. 11 as a function of m_{e_4} for three choices of couplings $g_L^h = 0.1, 0.05, 0.01$ with $g_L^Z = 0.01, g_R^h = g_R^Z = 0$. It is assumed that $\mathrm{BR}(e_4^\pm \to Z\mu^\pm) = 1$. We used the k factor 2.62 in order to match the leading order result for $\sigma(gg \to h)$ obtained from MadGraph 5 with the value presented by the Higgs Working Group [17] which includes higher order contributions. We use the same factor to multiply the cross section for $gg \to h \to Z\mu^+\mu^- \to 4\mu$ obtained from MadGraph 5 now including the

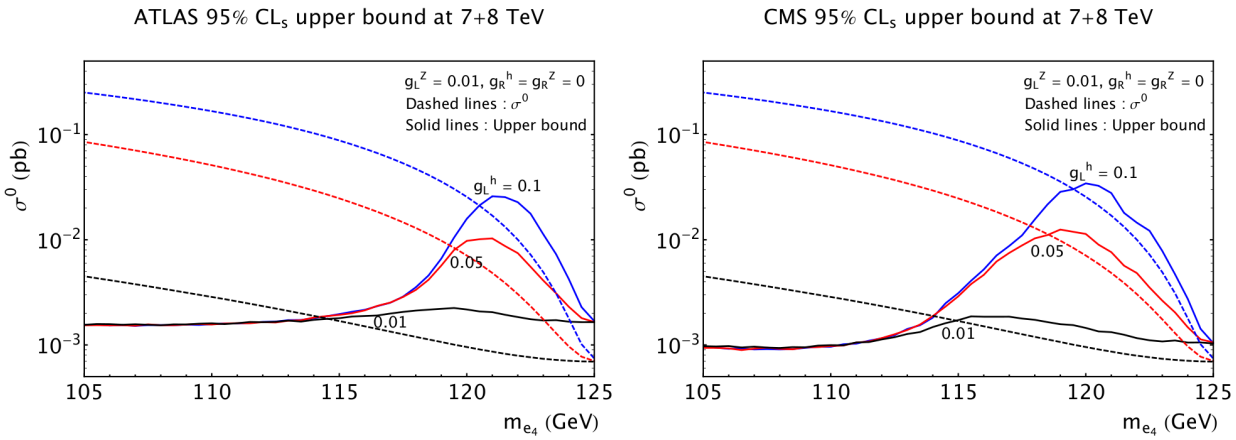
ATLAS 95% CL$_s$ upper bound at 7+8 TeV
CMS 95% CL$_s$ upper bound at 7+8 TeV
$g_L^Z = 0.01, g_R^h = g_R^Z = 0$
Dashed lines : σ^0
Solid lines : Upper bound
$g_L^h = 0.1$
0.05
0.01
σ^0 (pb)
m_{e_4} (GeV)

FIG. 11: Predicted cross section σ^0 for $gg \to h \to Z\mu^+\mu^- \to 4\mu$ as a function of m_{e_4} for $g_L^h = 0.1, 0.05, 0.01$ (dashed lines from top to bottom) and with $g_L^Z = 0.01, g_R^h = g_R^Z = 0$. The corresponding 95 % C.L. limits from the ATLAS (left) and CMS (right) analyses are indicated by solid lines.

contribution from the new lepton. The cross section of the SM $h \to ZZ^* \to 4\mu$ process $\sigma^0_{\rm SM}$ before applying the cuts is obtained from Ref. [17]. The derived 95 % C.L. upper limits on σ^0 from the ATLAS (left) and CMS (right) analyses for each choice of the g_L^h coupling are indicated by solid lines in Fig. 11. The bounds are inversely proportional to ξ.

Finally, we also analyzed the impact of constraints from $h \to WW^* \to 2\ell 2\nu$ on $h \to e_4^\pm \mu^\mp \to W^\pm \mu^\mp \nu$. The predicted cross sections for $gg \to h \to W^\pm \mu^\mp \nu_\mu \to \mu^+\mu^- 2\nu_\mu$ and $e^\pm \mu^\mp \nu_e \nu_\mu$ as functions of m_{e_4} for selected values of g_L^h are given in Fig. 12. The corresponding 95 % C.L. limits from the CMS analysis [22] are indicated by solid lines. They are obtained following the procedure discussed in detail in Ref. [16]. For each final state the events are further categorized according to the number of external jets mainly from the initial state radiations. Among them the strongest bound is selected for each value of m_{e_4}.

The constraints from $h \to WW^* \to 2\ell 2\nu$ on the new vectorlike lepton are typically weaker than those from $h \to ZZ^* \to 4\ell$, unless BR$(e_4^\pm \to W^\pm \nu)$ is close to 1. Thus these constraints are relevant only in a limited region of the parameter space. This is illustrated in Fig. 13 where we plot the points from Fig. 9 (left) that satisfy the ATLAS limit $R_{Z\mu\mu} < 2.8$ in $g_h \sqrt{\text{BR}(e_4 \to W\nu)}$ – m_{e_4} plane. The approximate limit on $\mu \equiv \sigma/\sigma_{\rm SM}$ for $e^\pm \mu^\mp \nu_e \nu_\mu$ final state (which is stronger than the limit for $2\mu 2\nu_\mu$ final state) is indicated by a thick (red) line. Only few points not excluded by $h \to ZZ^* \to 4\ell$ are excluded by $h \to WW^* \to 2\ell 2\nu$.

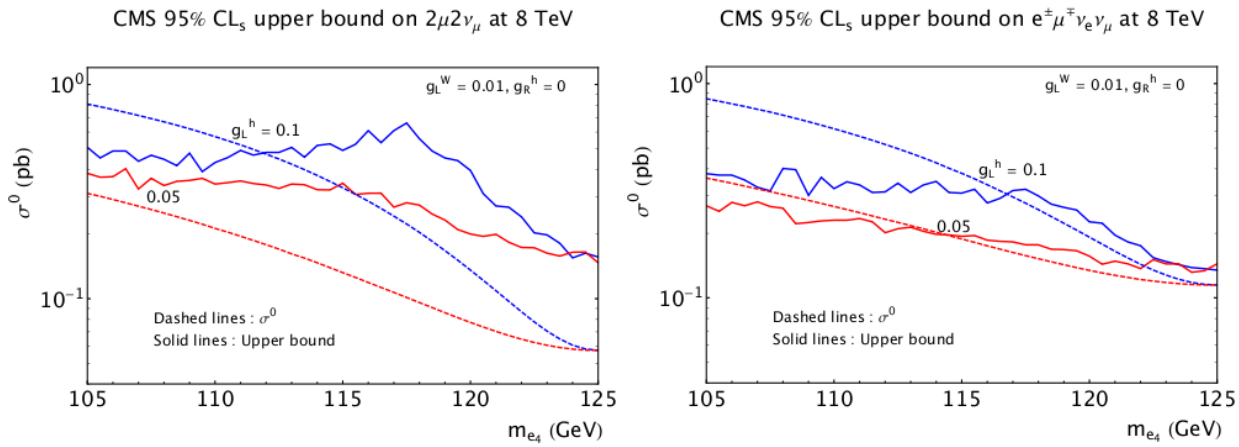
CMS 95% CL$_s$ upper bound on $2\mu 2\nu_\mu$ at 8 TeV
CMS 95% CL$_s$ upper bound on $e^\pm\mu^\mp\nu_e\nu_\mu$ at 8 TeV
$g_L^W = 0.01, g_R^h = 0$
$g_L^h = 0.1$
0.05
Dashed lines : σ^0
Solid lines : Upper bound
σ^0 (pb)
m_{e_4} (GeV)

FIG. 12: Predicted cross sections σ^0 for $gg \to h \to W^\pm\mu^\mp\nu_\mu \to \mu^+\mu^- 2\nu_\mu$ (left) and $e^\pm\mu^\mp\nu_e\nu_\mu$ (right) as functions of m_{e_4} for $g_L^h = 0.1, 0.05$ (dashed lines from top to bottom) and with $g_L^W = 0.01, g_R^h = 0$. The corresponding 95 % C.L. limits from the CMS analysis are indicated by solid lines as discussed in detail in Ref. [16].

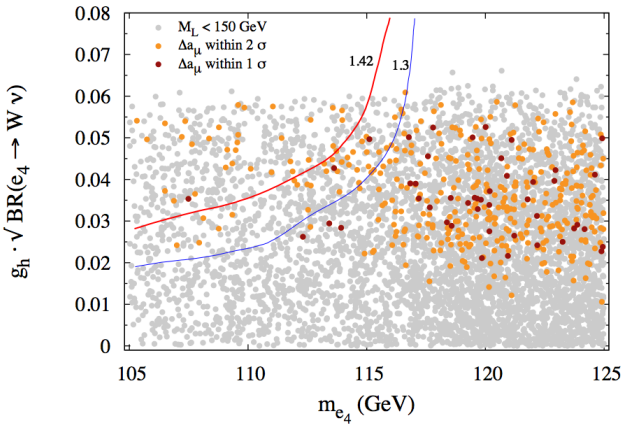

FIG. 13: Subset of points from Fig. 9 (left) that satisfy the ATLAS limit $R_{Z\mu\mu} < 2.8$ plotted in $g_h\sqrt{\text{BR}(e_4 \to W\nu)}$ – m_{e_4} plane. The thick (red) line indicates the limit on $\mu \equiv \sigma/\sigma_{\text{SM}}$ for $e^\pm\mu^\mp\nu_e\nu_\mu$ final state. In order to illustrate the impact of improved limits in the future we also show the contour of $\mu = 1.3$.

Appendix C: Partial width of $h \to Zf_1f_2$

In this Appendix we calculate the partial decay width of a scalar h decaying into Zf_1f_2 mediated by a new fermion f and the Z^*. This calculation can be straightforwardly modified for $h \to Wf_1f_2$. The relevant Feynman diagrams are shown in Fig. 14.

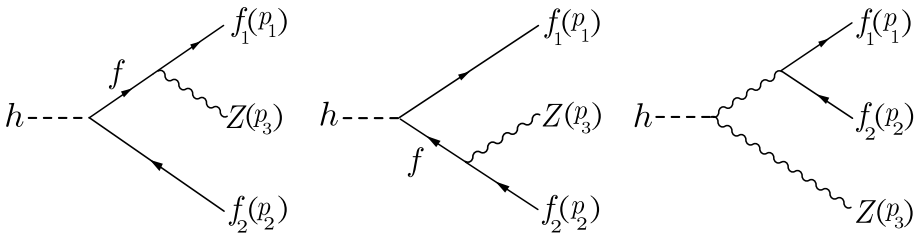

FIG. 14: Tree level Feynman diagrams for $h \to Z f_1 f_2$.

1. Amplitudes

The amplitudes for the three diagrams are:

$$iT_1 = \bar{u}_{f_1}(\mathbf{p_1})\frac{ig}{2c_W}\gamma^\mu(c_{v1}+c_{a1}\gamma_5)\frac{1}{i}\frac{\not{p}_1+\not{p}_3-m_f}{(p_1+p_3)^2+m_f^2-i\Gamma_f m_f}\frac{-i(y_{v1}+y_{a1}\gamma_5)}{2\sqrt{2}}v_{f_2}(\mathbf{p_2})\epsilon_\mu,$$

$$iT_2 = \bar{u}_{f_1}(\mathbf{p_1})\frac{-i(y_{v2}+y_{a2}\gamma_5)}{2\sqrt{2}}\frac{1}{i}\frac{\not{p}_2+\not{p}_3-m_f}{(p_2+p_3)^2+m_f^2-i\Gamma_f m_f}\gamma^\mu\frac{ig}{2c_W}(c_{v2}+c_{a2}\gamma_5)v_{f_2}(\mathbf{p_2})\epsilon_\mu,$$

$$iT_Z = \frac{-igM_Z}{c_W}\bar{u}_{f_1}(\mathbf{p_1})\gamma^\mu\frac{ig}{2c_W}(c_v+c_a\gamma_5)v_{f_2}(\mathbf{p_2})\frac{1}{i}\frac{g_{\mu\nu}}{(p_1+p_2)^2+M_Z^2-i\Gamma_Z M_Z}\epsilon^\nu(p_3), \qquad \text{(C1)}$$

where the notation for the couplings of the Z boson to fermions f and f_i follows from the Lagrangian, $\mathcal{L} \supset (g/2c_W)\bar{f}_i\gamma^\mu(c_{vi}+c_{ai}\gamma_5)fZ_\mu + h.c.$, and the couplings of the scalar are defined by $\mathcal{L} \supset -1/(2\sqrt{2})\bar{f}_i\gamma^\mu(y_{vi}+y_{ai}\gamma_5)fh + h.c.$.

Writing $k_{1,2} \equiv p_{1,2}+p_3$, the amplitude squared for the first diagram is given by

$$\begin{aligned}|T_1|^2 = {} & \frac{1}{8}\frac{g^2}{4c_W^2}\frac{1}{(k_1^2+m_f^2)^2+\Gamma_f^2 m_f^2}\epsilon_\mu(p_3)\epsilon_\nu^*(p_3) \\ & \mathrm{Tr}\left[u_{f_1}\bar{u}_{f_1}\gamma^\mu(c_{v1}+c_{a1}\gamma_5)(\not{k}_1-m_f)(y_{v1}+y_{a1}\gamma_5)v_{f_2}\bar{v}_{f_2}(y_{v1}-y_{a1}\gamma_5)(\not{k}_1-m_f)\gamma^\nu(c_{v1}+c_{a1}\gamma_5)\right].\end{aligned}$$

The polarization vectors ϵ_μ of the Z boson satisfy

$$\sum_{\lambda=\pm,0}\epsilon_\lambda^{*\rho}(k)\epsilon_\lambda^\sigma(k) = g^{\rho\sigma}+\frac{k^\rho k^\sigma}{M_Z^2}, \qquad \text{(C2)}$$

and summing over final spins, we get

$$\langle|T_1|^2\rangle = \sum_{\lambda=\pm,0}\sum_{f_1,f_2=\pm}|T_1|^2 = \frac{1}{8}\frac{g^2}{4c_W^2}\frac{1}{(k_1^2+m_f^2)^2+\Gamma_f^2 m_f^2}\left(g_{\mu\nu}+\frac{p_{3\mu}p_{3\nu}}{M_Z^2}\right)\mathcal{M}_1^{\mu\nu}, \qquad \text{(C3)}$$

where

$$\mathcal{M}_1^{\mu\nu} \;=\; \mathrm{Tr}[(-\not{p}_1 + m_1)\gamma^\mu(c_{v1} + c_{a1}\gamma_5)(\not{k}_1 - m_f)(y_{v1} + y_{a1}\gamma_5) \\ (-\not{p}_2 - m_2)(y_{v1} - y_{a1}\gamma_5)(\not{k}_1 - m_f)\gamma^\nu(c_{v1} + c_{a1}\gamma_5)]. \qquad \text{(C4)}$$

The $\langle|T_2|^2\rangle$ can be obtained from $\langle|T_1|^2\rangle$, by making the following replacements:

- $p_1 \leftrightarrow p_2$ and $m_1 \leftrightarrow -m_2$,
- $c_{v1} \to c_{v2}$, $c_{a1} \to c_{a2}$, $y_{v1} \to y_{v2}$ and $y_{a1} \to -y_{a2}$.

Interference between the two diagrams is given by twice the real part of

$$\langle T_1\bar{T}_2\rangle \;=\; \sum_{\lambda=\pm,0}\sum_{f_1,f_2=\pm} T_1\bar{T}_2 \\ \;=\; \frac{1}{8}\frac{g^2}{4c_W^2}\left(\frac{1}{k_1^2 + m_f^2 - i\Gamma_f m_f}\right)\left(\frac{1}{k_2^2 + m_f^2 - i\Gamma_f m_f}\right)^*\left(g_{\mu\nu} + \frac{p_{3\mu}p_{3\nu}}{M_Z^2}\right)\mathcal{M}_{12}^{\mu\nu},$$

where

$$\mathcal{M}_{12}^{\mu\nu} \;=\; \mathrm{Tr}[(-\not{p}_1 + m_1)\gamma^\mu(c_{v1} + c_{a1}\gamma_5)(\not{k}_1 - m_f)(y_{v1} + y_{a1}\gamma_5) \\ (-\not{p}_2 - m_2)\gamma^\nu(c_{v2} + c_{a2}\gamma_5)(\not{k}_2 - m_f)(y_{v2} - y_{a2}\gamma_5)]. \qquad \text{(C5)}$$

The interference with ZZ^* is given by $2\mathrm{Re}\langle T_1\bar{T}_Z\rangle + 2\mathrm{Re}\langle T_2\bar{T}_Z\rangle$, where

$$\langle T_1\bar{T}_Z\rangle \;=\; -\frac{g^3 M_Z}{8\sqrt{2}c_W^3}\frac{1}{k_1^2 + m_f^2 - i\Gamma_f m_f}\left(\frac{1}{(p_1+p_2)^2 + M_Z^2 - i\Gamma_Z M_Z}\right)^*\left(g_{\mu\nu} + \frac{p_{3\mu}p_{3\nu}}{M_Z^2}\right)\mathcal{M}_{1Z}^{\mu\nu}$$

with

$$\mathcal{M}_{1Z}^{\mu\nu} \;=\; \mathrm{Tr}[(-\not{p}_1 + m_1)\gamma^\mu(c_{v1} + c_{a1}\gamma_5)(\not{k}_1 - m_f)(y_{v1} + y_{a1}\gamma_5)(-\not{p}_2 - m_2)\gamma^\nu(c_v + c_a\gamma_5)], \qquad \text{(C6)}$$

and $\langle T_2\bar{T}_Z\rangle$ can be obtained from $\langle T_1\bar{T}_Z\rangle$ by making the same substitutions as for $\langle|T_2|^2\rangle$, listed above.

2. Traces

The results for the traces appearing in the amplitudes squared are:

$$\begin{aligned}
\mathcal{M}_1^{\mu\nu} g_{\mu\nu} &= 8({c_{v1}}^2 + {c_{a1}}^2)(y_{v1}^2 + y_{a1}^2)\left(2(p_1k_1)(k_1p_2) - (p_1p_2)k_1^2 - m_f^2(p_1p_2)\right) \\
&+ 16m_f m_2({c_{v1}}^2 + {c_{a1}}^2)(y_{v1}^2 - y_{a1}^2)\,(p_1k_1) + 32m_1 m_f({c_{v1}}^2 - {c_{a1}}^2)(y_{v1}^2 + y_{a1}^2)(k_1p_2) \\
&- 16m_1 m_2({c_{v1}}^2 - {c_{a1}}^2)(y_{v1}^2 - y_{a1}^2)(k_1^2 - m_f^2) \\
&- 32c_{v1}c_{a1}y_{v1}y_{a1}\left(2(p_1k_1)(k_1p_2) - (p_1p_2)k_1^2 + m_f^2(p_1p_2)\right), \qquad \text{(C7)}
\end{aligned}$$

$$\begin{aligned}
\mathcal{M}_1^{\mu\nu} p_{3\mu}p_{3\nu} &= 4(({c_{v1}}^2 + {c_{a1}}^2)(y_{v1}^2 + y_{a1}^2) - 4c_{v1}c_{a1}y_{v1}y_{a1}) \\
&\qquad \{-4(p_1p_3)(k_1p_2)(k_1p_3) + 2(p_1p_3)k_1^2(p_2p_3) - 2(p_1k_1)(p_2k_1)M_Z^2 + (p_1p_2)k_1^2M_Z^2\} \\
&+ 4m_f^2(({c_{v1}}^2 + {c_{a1}}^2)(y_{v1}^2 + y_{a1}^2) + 4c_{v1}c_{a1}y_{v1}y_{a1})\left\{2(p_1p_3)(p_3p_2) + (p_1p_2)M_Z^2\right\} \\
&- 8m_f m_2({c_{v1}}^2 + {c_{a1}}^2)(y_{v1}^2 - y_{a1}^2)\left\{2(p_1p_3)(p_3k_1) + (p_1k_1)M_Z^2\right\} \\
&+ 4m_1m_2M_Z^2({c_{v1}}^2 - {c_{a1}}^2)(y_{v1}^2 - y_{a1}^2)k_1^2 - 8m_1m_fM_Z^2({c_{v1}}^2 - {c_{a1}}^2)(y_{v1}^2 + y_{a1}^2)(p_2k_1) \\
&- 4m_1m_2m_f^2M_Z^2({c_{v1}}^2 - {c_{a1}}^2)(y_{v1}^2 - y_{a1}^2), \qquad \text{(C8)}
\end{aligned}$$

$$\begin{aligned}
\mathcal{M}_{12}^{\mu\nu} g_{\mu\nu} &= 16(c_{v1}c_{v2} - c_{a1}c_{a2})y_{v1}y_{v2}((k_1p_2) + m_fm_2)\,(-p_1k_2 + m_1m_f) \\
&\quad - 8(c_{v1}c_{v2} + c_{a1}c_{a2})y_{v1}y_{v2}\left(-m_1m_2(k_1k_2) + m_1m_f(p_2k_2) - m_2m_f(k_1p_1) + m_f^2(p_1p_2)\right) \\
&\quad -16(c_{v1}c_{v2} - c_{a1}c_{a2})y_{a1}y_{a2}((k_1p_2) - m_fm_2)\,((p_1k_2) + m_1m_f) \\
&\quad + 8(c_{v1}c_{v2} + c_{a1}c_{a2})y_{a1}y_{a2}\left(-m_2m_1(k_1k_2) - m_fm_1(p_2k_2) + m_fm_2(p_1k_1) + m_f^2(p_1p_2)\right), \\
&\quad -16(c_{v1}c_{a2} - c_{a1}c_{v2})(y_{v1}y_{a2} + y_{a1}y_{v2})\left((p_1k_2)(k_1p_2) + m_1m_2m_f^2\right) \\
&\quad -8(c_{v1}c_{a2} + c_{a1}c_{v2})(y_{v1}y_{a2} + y_{a1}y_{v2})m_f\,(m_1(p_2k_2) + m_2(p_1k_1)) \\
&\quad -8(c_{v1}c_{a2} + c_{a1}c_{v2})(y_{v1}y_{a2} - y_{a1}y_{v2})\left(m_1m_2(k_1k_2) - m_f^2(p_1p_2)\right) \\
&\quad +8(c_{v1}c_{a2} - c_{a1}c_{v2})(y_{v1}y_{a2} - y_{a1}y_{v2})\,(m_fm_2(p_1k_2) + m_1m_f(k_1p_2)), \qquad \text{(C9)}
\end{aligned}$$

$$
\begin{aligned}
\mathcal{M}_{12}^{\mu\nu} p_{3\mu} p_{3\nu} \;=\; & 4\left((c_{v1}c_{v2}-c_{a1}c_{a2})(y_{v1}y_{v2}+y_{a1}y_{a2})+(c_{v1}c_{a2}-c_{a1}c_{v2})(y_{v1}y_{a2}+y_{a1}y_{v2})\right) \\
& \{(k_2p_1)(k_1p_2)M_Z^2-2(k_2p_3)(2(p_1p_2)(k_1p_3)-(p_1k_1)(p_2p_3)) \\
& -(k_2k_1)(2(p_1p_3)(p_3p_2)+(p_1p_2)M_Z^2)+(k_2p_2)(2(p_1p_3)(p_3k_1)+(p_1k_1)M_Z^2)\} \\
- \; & 4\left((c_{v1}c_{v2}+c_{a1}c_{a2})(y_{v1}y_{v2}+y_{a1}y_{a2})-(c_{v1}c_{a2}+c_{a1}c_{v2})(y_{v1}y_{a2}+y_{a1}y_{v2})\right) \\
& m_f m_2\left(2(p_1p_3)(p_3k_1)+(p_1k_1)M_Z^2\right) \\
+ \; & 4\left((c_{v1}c_{v2}+c_{a1}c_{a2})(y_{v1}y_{v2}-y_{a1}y_{a2})-(c_{v1}c_{a2}+c_{a1}c_{v2})(y_{v1}y_{a2}-y_{a1}y_{v2})\right) \\
& m_f^2\left(2(p_1p_3)(p_3p_2)+(p_1p_2)M_Z^2\right) \\
+ \; & 4\left((c_{v1}c_{v2}-c_{a1}c_{a2})(y_{v1}y_{v2}-y_{a1}y_{a2})-(c_{v1}c_{a2}-c_{a1}c_{v2})(y_{v1}y_{a2}-y_{a1}y_{v2})\right) \\
& M_Z^2 m_f m_2(p_1k_2) \\
- \; & 4\left((c_{v1}c_{v2}-c_{a1}c_{a2})(y_{v1}y_{v2}-y_{a1}y_{a2})-(c_{v1}c_{a2}-c_{a1}c_{v2})(y_{v1}y_{a2}-y_{a1}y_{v2})\right) \\
& M_Z^2 m_f m_1(k_1p_2) \\
- \; & 4\left((c_{v1}c_{v2}+c_{a1}c_{a2})(y_{v1}y_{v2}-y_{a1}y_{a2})-(c_{v1}c_{a2}+c_{a1}c_{v2})(y_{v1}y_{a2}-y_{a1}y_{v2})\right) \\
& m_1 m_2\left(2(p_3k_2)(p_3k_1)+M_Z^2(k_1k_2)\right) \\
+ \; & 4\left((c_{v1}c_{v2}+c_{a1}c_{a2})(y_{v1}y_{v2}+y_{a1}y_{a2})+(c_{v1}c_{a2}+c_{a1}c_{v2})(y_{v1}y_{a2}+y_{a1}y_{v2})\right) \\
& m_1 m_f\left(2(p_3k_2)(p_3p_2)+M_Z^2(p_2k_2)\right) \\
- \; & 4\left((c_{v1}c_{v2}-c_{a1}c_{a2})(y_{v1}y_{v2}+y_{a1}y_{a2})-(c_{v1}c_{a2}-c_{a1}c_{v2})(y_{v1}y_{a2}+y_{a1}y_{v2})\right) \\
& m_1 m_2 m_f^2 M_Z^2, \qquad \text{(C10)}
\end{aligned}
$$

$$
\begin{aligned}
\mathcal{M}_{1Z}^{\mu\nu} g_{\mu\nu} \;=\; & -8c_v y_{v1} c_{v1}(2m_1(k_1p_2)+2m_1m_2m_f+m_2(p_1k_1)-m_f(p_1p_2)) \\
+ \; & 8c_a y_{v1} c_{a1}(2m_1(k_1p_2)+2m_1m_2m_f-m_2(p_1k_1)+m_f(p_1p_2)) \\
- \; & 8c_a y_{a1} c_{v1}(2m_1(k_1p_2)-2m_1m_2m_f-m_2(p_1k_1)-m_f(p_1p_2)) \\
+ \; & 8c_v y_{a1} c_{a1}(2m_1(k_1p_2)-2m_1m_2m_f+m_2(p_1k_1)+m_f(p_1p_2)), \qquad \text{(C11)}
\end{aligned}
$$

$$
\begin{aligned}
&\mathcal{M}_{1Z}^{\mu\nu} p_{3\mu} p_{3\nu} = \\
&4c_v c_{v1} y_{v1} \left(m_1 M_Z^2 (k_1 p_2 + m_2 m_f) + m_2 (2(p_3 k_1)(p_1 p_3) + (p_1 k_1) M_Z^2) - m_f (2(p_1 p_3)(p_2 p_3) + p_1 p_2 M_Z^2)\right) \\
-\ &4c_a c_{a1} y_{v1} \left(m_1 M_Z^2 (k_1 p_2 + m_2 m_f) - m_2 (2(p_3 k_1)(p_1 p_3) + (p_1 k_1) M_Z^2) + m_f (2(p_1 p_3)(p_2 p_3) + p_1 p_2 M_Z^2)\right) \\
+\ &4c_a c_{v1} y_{a1} \left(m_1 M_Z^2 (k_1 p_2 - m_2 m_f) - m_2 (2(p_3 k_1)(p_1 p_3) + (p_1 k_1) M_Z^2) - m_f (2(p_1 p_3)(p_2 p_3) + p_1 p_2 M_Z^2)\right) \\
-\ &4c_v c_{a1} y_{a1} \left(m_1 M_Z^2 (k_1 p_2 - m_2 m_f) + m_2 (2(p_3 k_1)(p_1 p_3) + (p_1 k_1) M_Z^2) + m_f (2(p_1 p_3)(p_2 p_3) + p_1 p_2 M_Z^2)\right).
\end{aligned}
\tag{C12}
$$

3. Kinematics

The higgs 4-momentum is denoted by $P = p_1 + p_2 + p_3$. Defining $s_i = -(P - p_i)^2$ for i=1 to 3, we also have $\sum_i s_i = M_h^2 + M_Z^2 + m_1^2 + m_2^2$. Therefore the scalar products of the momenta are:

$$
\begin{aligned}
2p_1p_2 &= s_1 + s_2 - M_h^2 - M_Z^2, \\
2p_1p_3 &= -s_2 + m_1^2 + M_Z^2, \\
2p_2p_3 &= -s_1 + m_2^2 + M_Z^2.
\end{aligned}
\tag{C13}
$$

Substituting these into the amplitudes squared, we can integrate over $s_{1,2}$. The decay rate is given by

$$
\Gamma = \frac{1}{(2\pi)^3} \frac{1}{32 M_h^3} \int_{s_1^-}^{s_1^+} \int_{s_2^-}^{s_2^+} \langle |T|^2 \rangle \, ds_1 ds_2,
\tag{C14}
$$

with the limits defined as in [23], [24]:

$$
\begin{aligned}
s_1^- &= (m_2 + M_Z)^2, \\
s_1^+ &= (M_h - m_1)^2, \\
s_2^- &= m_1^2 + M_Z^2 + \frac{1}{2s_1}((M_h^2 - s_1 - m_1^2)(s_1 - m_2^2 + M_Z^2) - \lambda(s_1, M_h^2, m_1^2)\lambda(s_1, m_2^2, M_Z^2)), \\
s_2^+ &= m_1^2 + M_Z^2 + \frac{1}{2s_1}((M_h^2 - s_1 - m_1^2)(s_1 - m_2^2 + M_Z^2) + \lambda(s_1, M_h^2, m_1^2)\lambda(s_1, m_2^2, M_Z^2)),
\end{aligned}
$$

where $\lambda(x, y, z) = (x^2 + y^2 + z^2 - 2xy - 2yz - 2zx)^{1/2}$.

The $h \to Z\mu^+\mu^-$ can be obtained from the formulas above by substituting $f_1 = f_2 = \mu$, $f = e_4$,

and

$$
\begin{aligned}
c_{v1} = c_{v2} &= \frac{c_W}{g}(g_L^Z + g_R^Z), \\
c_{a1} = c_{a2} &= \frac{c_W}{g}(-g_L^Z + g_R^Z), \\
y_{v1} = y_{v2} &= g_L^h + g_R^h, \\
y_{a1} = y_{a2} &= -g_L^h + g_R^h,
\end{aligned}
$$

to match the notation in Eq. (3).

4. $h \to Wtb$

As a special case, in order to check and illustrate the usefulness of the general formulas, we calculate the partial decay width of the Higgs boson into Wtb in the SM. There is only one diagram in this case since the contribution from WW^* is negligible. To get this result from our calculation, we make the following replacements:

- $M_Z \to M_W$,
- $m_{1,2} \to m_{b,t}$ and $m_f = m_t$,
- $\frac{g}{2c_W} \to \frac{g}{\sqrt{2}}$ and $c_{v1} = -c_{a1} = 1/2$,
- $\frac{y_{v1}}{2\sqrt{2}} \to \frac{m_t}{v}$ and $\frac{y_{a1}}{2\sqrt{2}} \to 0$,

where v = 174 GeV. The amplitude squared is

$$
\langle |T_1|^2 \rangle = \frac{g^2 m_t^2}{2v^2} \frac{1}{(-s_2 + m_t^2)^2 + \Gamma_t^2 m_t^2} \left(g_{\mu\nu} + \frac{p_{3\mu} p_{3\nu}}{M_W^2} \right) \mathcal{M}_1^{\mu\nu} \equiv \frac{g^2 m_t^2}{2v^2} \frac{M_h^2}{M_W^2} \frac{\Gamma_0}{y_t^2 + \gamma_t \kappa_t}, \quad \text{(C15)}
$$

where we have defined: $\Gamma_0 \equiv \left(\kappa_W \frac{g_{\mu\nu}}{M_h^4} + \frac{p_{3\mu} p_{3\nu}}{M_h^6} \right) \mathcal{M}_1^{\mu\nu}$, $x_{t,b} = \frac{2E_{t,b}}{M_h}$, $y_{t,b} = 1 - x_{t,b}$, $\kappa_W = \frac{m_W^2}{M_h^2}$, $\kappa_t = \frac{m_t^2}{M_h^2}$, and $\gamma_t = \frac{\Gamma_t^2}{M_h^2}$. Using these definitions, $s_{1,2}$ can be written as:

$$
\begin{aligned}
s_1 &= -P^2 - p_1^2 + 2P \cdot p_1 = M_h^2 + m_b^2 - 2M_h E_b \approx M_h^2 \left(1 - \frac{2E_b}{M_h} \right) \equiv M_h^2 y_b, \\
s_2 &= -P^2 - p_2^2 + 2P \cdot p_2 = M_h^2 + m_t^2 - 2M_h E_t = M_h^2 \left(1 - \frac{2E_t}{M_h} + \frac{m_t^2}{M_h^2} \right) \equiv M_h^2 y_t + m_t^2, \quad \text{(C16)}
\end{aligned}
$$

where m_b is neglected. With $ds_1 = -2M_h dE_b$ and $ds_2 = -2M_h dE_t$, the differential decay width can be written as

$$
d\Gamma = \frac{N_c}{(2\pi)^3} \frac{1}{8M_h} \langle |T|^2 \rangle \, dE_b dE_t = \frac{N_c G_F^2}{64\pi^3} m_t^2 M_h^3 \frac{\Gamma_0}{y_t^2 + \gamma_t \kappa_t} \, dx_b dx_t, \quad \text{(C17)}
$$

where $G_F = g/(4vM_W)$. This result agrees with the formula in Ref. [25].

---

[1] ATLAS Collaboration, ATLAS-CONF-2013-013.

[2] S. Chatrchyan *et al.* [CMS Collaboration], arXiv:1312.5353 [hep-ex].

[3] K. Kannike, M. Raidal, D. M. Straub and A. Strumia, JHEP **1202**, 106 (2012) [arXiv:1111.2551 [hep-ph]].

[4] R. Dermisek and A. Raval, Phys. Rev. D **88**, 013017 (2013) [arXiv:1305.3522 [hep-ph]].

[5] G. Blankenburg, J. Ellis and G. Isidori, Phys. Lett. B **712**, 386 (2012) [arXiv:1202.5704 [hep-ph]].

[6] R. Harnik, J. Kopp and J. Zupan, JHEP **1303**, 026 (2013) [arXiv:1209.1397 [hep-ph]].

[7] S. A. R. Ellis, R. M. Godbole, S. Gopalakrishna and J. D. Wells, arXiv:1404.4398 [hep-ph].

[8] R. Dermisek, Phys. Lett. B **713**, 469 (2012) [arXiv:1204.6533 [hep-ph]].

[9] R. Dermisek, Phys. Rev. D **87**, 055008 (2013) [arXiv:1212.3035 [hep-ph]].

[10] G. W. Bennett *et al.* [Muon G-2 Collaboration], Phys. Rev. D **73**, 072003 (2006) [hep-ex/0602035].

[11] CMS Collaboration, CMS-PAS-HIG-13-007.

[12] R. Dermisek, J. P. Hall, E. Lunghi and S. Shin, arXiv:1408.3123 [hep-ph].

[13] M. Gonzalez-Alonso and G. Isidori, Phys. Lett. B **733**, 359 (2014) [arXiv:1403.2648 [hep-ph]].

[14] A. Falkowski and R. Vega-Morales, arXiv:1405.1095 [hep-ph].

[15] CERN Yellow report 2000-205; ATLAS and CMS Collaborations, LHC Higgs Combination Group, "Procedure for the LHC Higgs boson search combination in Summer 2011", ATL-PHYS-PUB/CMS-NOTE 2011-11, 2011/005 (2011).

[16] R. Dermisek, J. P. Hall, E. Lunghi and S. Shin, JHEP **1404**, 140 (2014) [arXiv:1311.7208 [hep-ph]].

[17] S. Heinemeyer *et al.* [LHC Higgs Cross Section Working Group Collaboration], arXiv:1307.1347 [hep-ph].

[18] G. Aad *et al.* [ATLAS Collaboration], arXiv:1406.3827 [hep-ex].

[19] J. Alwall, R. Frederix, S. Frixione, V. Hirschi, F. Maltoni, O. Mattelaer, H. -S. Shao and T. Stelzer *et al.*, arXiv:1405.0301 [hep-ph].

[20] A. Alloul, N. D. Christensen, C. Degrande, C. Duhr and B. Fuks, Comput. Phys. Commun.

185, 2250 (2014) [arXiv:1310.1921 [hep-ph]] ; C. Degrande, C. Duhr, B. Fuks, D. Grellscheid, O. Mattelaer and T. Reiter, Comput. Phys. Commun. **183**, 1201 (2012) [arXiv:1108.2040 [hep-ph]].

[21] T. Sjostrand, S. Mrenna and P. Z. Skands, JHEP **0605**, 026 (2006) [hep-ph/0603175].

[22] CMS Collaboration, CMS-PAS-HIG-13-003.

[23] J. Beringer et al. (Particle Data Group), Phys. Rev. D86, 010001 (2012) and 2013 partial update for the 2014 edition

[24] W. von Schlippe, *Relativistic Kinematics of Particle Interactions*, `http://www.helsinki.fi/~www_sefo/phenomenology/`

[25] A. Djouadi, Phys. Rept. **457**, 1 (2008) [hep-ph/0503172].